

REDUCTIONS IN BERM HEIGHT AND FORESHORE SLOPE DUE TO FILTRATION FLOW ON GRAVEL BEACH

Takaaki Uda¹, Masumi Serizawa², Mitsunaga Okamoto³, Toshinori Ishikawa⁴,
Yasuhito Noshi⁵ and Shiho Miyahara²

The closure mechanism of the mouth of a floodway owing to the deposition of gravel by waves was investigated, taking the Shin-nakagawa floodway flowing into the Fuji coast as an example. A movable bed experiment with a model scale of 1/50 using a two-dimensional wave channel was carried out, while changing the discharge of the floodway. It was found that the berm height and foreshore slope were reduced owing to the filtration flow on the gravel beach. A model for predicting beach changes with filtration flow based on the contour-line-change model was proposed. The effect of the filtration flow on the cross-shore sand transport was incorporated in the model, and the calculation results were in good agreement with the experimental results.

Keywords: filtration flow; gravel beach; berm height; equilibrium slope; experiment; contour-line-change model

INTRODUCTION

In a floodway for a drainage extending across sandy beaches exposed to the open sea, the mouth of the floodway is often closed by sand deposition due to waves. On these coasts, a high berm develops in general because of a large incident wave height, and this causes the full closure of the mouth of the floodway. At the Shin-nakagawa floodway flowing into the Fuji coast, the floodway is successfully maintained even though high waves are often incident during storms. The field observation of this floodway showed that reductions in berm height and foreshore slope were assumed to occur under the condition that filtration flow exists, and this is supposed to be a mechanism of the drainage free from maintenance. Such effect, however, has not yet been investigated. In addition to the field observation of the Shin-nakagawa floodway, a movable-bed experiment with a scale of 1/50 using a two-dimensional wave channel was carried out. As a result, it was suggested that the foreshore slope and berm height could be decreased with the increase in the amount of discharge from the floodway, as an effect of the filtration flow to the cross-shore sand transport. Such effect could be explained by the mechanism that the equilibrium slope of sand, which is determined by the balance between the intensities of outgoing and incoming waves (Serizawa et al. 2003), decreases under the condition that waves and filtration flow coexist. In this study, a model for predicting beach changes was developed, taking the effect of the filtration flow into account using the contour-line-change model proposed by Serizawa et al. (2003), and numerical simulation results were compared with those obtained by the experiment.

OBSERVATION AT SHIN-NAKAGAWA FLOODWAY

Figure 1 shows the satellite image of the Shin-nakagawa floodway on the Fuji coast. This floodway is composed of old and new floodways on the east and west sides, respectively, with a horseshoe or rectangular mouth, and they extend obliquely to the direction normal to the shoreline. In Fig. 1, a stream flowing from the mouth of the old floodway can be observed on the east side with a pond in front of the mouth, and this pond has been completely closed by a sand bar of 12 m width, and no channel connects between the pond and the sea. A discharge of approximately 0.8 m³/s continuously flowed down to the sea during the day, implying that all the drainage from the floodway discharged as the filtration flow across the sand bar. On the other hand, in front of the floodway, a slightly concave shoreline is observed, and this might closely be related to the filtration flow crossing the sand bar. Therefore, in the field observation, this point was investigated in detail.

Figure 2 shows the detailed condition of the floodways. The old floodway faces approximately normal to the shoreline, whereas the new one extends normal to the direction of the old floodway. A large amount of gravel was deposited in front of the new floodway, and almost half of the mouth was buried with gravel. In front of the old floodway, the drainage from the floodway rapidly filtrated into

¹ Head, Shore Protection Research, Public Works Research Center, 1-6-4 Taito, Taito, Tokyo 110-0016, Japan

² Coastal Engineering Laboratory Co., Ltd., 1-22-301 Wakaba, Shinjuku, Tokyo 160-0011, Japan

³ Numazu Public Works Office, Shizuoka Prefectural Government, 1-3 Takashima-honmachi, Numazu, Shizuoka 410-0055, Japan

⁴ Public Works Research Center, 1-6-4 Taito, Taito, Tokyo 110-0016, Japan

⁵ Nihon University, 7-24-1 Narashinodai, Funabashi, Chiba 274-8501, Japan

the gravel layer near the mouth. Here, the elevation of the mouth is +0.34 m above the mean sea level (MSL). As typical wave conditions of storm waves with a probability of occurrence of once a year on this coast, the significant wave height $H_{1/3}$ ranges between 2 and 3 m and the wave period $T_{1/3}$ is 11 s.



Figure 1. Satellite image of Shin-nakagawa floodway taken on January 9, 2015.



Figure 2. Horseshoe and rectangular mouths of old and new Shin-nakagawa floodways, respectively, and deposition of gravel in front of the mouths.

Figure 3 shows the old floodway and the pond formed in front of the mouth. The drainage from the old floodway flowed eastward, and then all discharge filtrated into the gravel layer. Although a high berm **A** was formed immediately east of the old floodway, the south side of this berm was truncated by the steep slope **B** of the angle of repose of gravel, which was formed by the erosion on the side slope by strong currents during a flood. A berm was formed in front of the old floodway, but the height of the berm was much smaller than the berm height on the nearby beach. Figure 4 shows the shoreline where the water filtrated from the pond in front of the old floodway flows out to the sea. In the vicinity of this location, a concave shoreline was formed together with an upward concave profile of the beach face. This is in good agreement with the fact that a concave shoreline was observed in

front of the floodway, as shown in Fig. 1. Figure 5 shows the beach material deposited in front of the old floodway, and the beach was composed of gravel of grain size ranging between 5 and 10 cm.



Figure 3. Mouth of old floodway and a pond in front of the mouth.



Figure 4. Concave shoreline where filtration water flows out into sea.



Figure 5. Grain size of beach material composing berm.

In the field observation, the berm height and foreshore slope were measured in the vicinity of the floodway. First, the berm height immediately east of the floodway was +3 m above MSL, as shown in Fig. 6, whereas that in front of the old floodway was +2.1 m, as shown in Fig. 7, i.e., 0.9 m lower than the berm height of the natural sandy beach. As for the foreshore slope, the slope was 1/2.5 immediately west of the old floodway (Fig. 8). In contrast, the foreshore slope at a location where filtration flow discharged out to the sea was 1/4 (Fig. 9), and thus the reduction of the foreshore slope was confirmed. Furthermore, strong return currents to the sea were observed in the central part of a concave shoreline, as shown in Fig. 10, as in the case near the apex of the beach cusps (Shibasaki et al. 2004), and a reduction in the height of the incoming waves was observed because of strong offshore return currents concentrated at the central part. Finally, it was confirmed that the berm height and foreshore slope were reduced at a location where filtration flow on the gravel beach discharged out to sea, resulting in the formation of a concave shoreline, as mentioned above. In reference to the concept of the equilibrium slope as described by Serizawa et al. (2003), the seaward filtration flow is assumed to intensify the action of outgoing waves, resulting in the reduction of the beach slope. Thus, filtration flow on the gravel beach is assumed to decrease in equilibrium slope, and beach changes occur so that the foreshore slope and berm height are reduced.



Figure 6. Berm height of 3 m above MSL immediately east of the floodway.



Figure 7. Berm height of 2.1 m above MSL in front of the mouth of old floodway.



Figure 8. Foreshore slope of 1/2.5 at natural beach.



Figure 9. Foreshore slope of 1/4 at a location where filtration water discharges out to sea.



Figure 10. Concentrated seaward currents associated with filtration flow.

METHOD OF EXPERIMENT

A two-dimensional movable bed experiment was carried out to investigate the mechanism of the reductions in berm height and foreshore slope observed at the Shin-nakagawa floodway. A wave tank

of 8 m length, 0.4 m width and 35 cm depth was used for the experiment, and a model beach with the initial slope of 1/5 was produced using gravel with the median diameter d_{50} of 3.3 mm. By setting the model scale as 1/50, regular waves became incident to the model beach. Variables were determined so as to satisfy Froude's similarity. Meshes at 10 cm intervals were drawn on the side glass of the wave channel, as shown in Fig. 11, and the longitudinal profile was measured by photographing from the side glass.

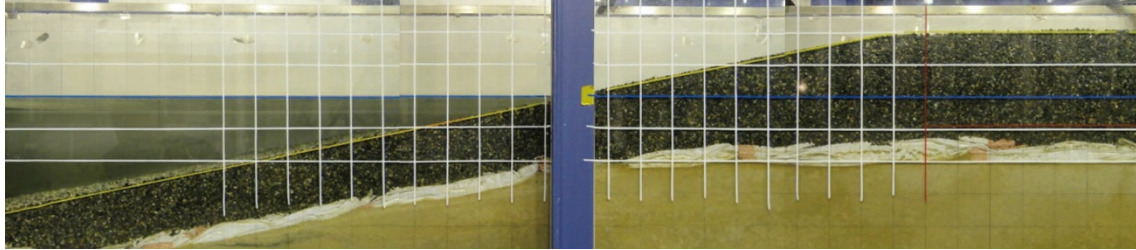


Figure 11. Wave flume and initial beach profile.

In a small-scale experiment, characteristic beach changes occur, and the type of profile changes can be classified, depending on the C -parameter proposed by Horikawa (1988), using the grain size d of sand, the wave height H , the wave period T and the beach slope $\tan\beta$.

$$H_0/L_0 = C (\tan\beta)^{-0.27} (d/L_0)^{0.67} \quad (1)$$

In Eq. (1), sand is considered to be transported shoreward to form a berm if C is smaller than 4, whereas seaward sand transport dominates and the foreshore will be eroded if C is greater than 8. In this study, sand deposition in front of the floodway mouth is important, and thus the condition in which shoreward sand transport is predominant was adopted. Regular waves were employed in the experiment.

First, as a preliminary test of the beach changes, the wave condition for the berm height to be 6 cm (3 m in the prototype) was tested, and a wave height of 3 cm and a wave period of 1.3 s were selected. This experimental condition corresponds to the waves of $H = 1.5$ m and $T = 9.2$ s in the prototype. Furthermore, the duration of the experiment was determined to be 3 h, because the berm has sufficiently developed after a 3-hour wave generation. Table 1 shows the experimental conditions.

Table 1. Conditions of experiment.	
Facility	Two-dimensional wave tank: 8 m length, 0.4 m width and 0.35 cm depth
Method of experiment	Movable bed experiment: reproduction of berm height of 6 cm
Model scale	1/50
Duration of experiment	3 hrs
Wave conditions	Regular waves: $H_m = 3$ cm, $T_m = 1.3$ s ($H = 1.5$ m and $T = 9.2$ s in the prototype)
Grain size	Median diameter $d_{50} = 3.3$ mm.
Model beach	Movable bed: Initial slope of 1/5
Model floodway	Acrylic resin: 30 cm length, 10 cm width and 7.1 cm height Elevation of the basement of the floodway: 4.5 cm below MSL

In the experiment, a model floodway of 10 cm width and made of acrylic resin was installed along the side wall of the wave channel, and the longitudinal profile was measured on the side glass by tracing the profile. When the mouth of the floodway is set at the shoreline, a large amount of sand is deposited, and thus the mouth was set back by 50 cm (25 m in the prototype) from the shoreline landward of the berm top. The elevation of the basement of the floodway was set to be 4.5 cm below MSL. The discharge of the floodway was kept constant using a water pump, as schematically shown in Fig. 12. Figure 13 shows the side view and overview of the wave tank. A constant discharge was given under the wave condition in which a berm height of 6 cm is reproduced. As the discharge in the experiment, $Q_m = 17$ l/min in the experiment ($Q_p = 0.3$ m³/s in the prototype) was selected as the reference discharge, and Q_m was increased at six steps, as shown in Table 2. In addition, the inner water level behind the berm was measured using the photographs.

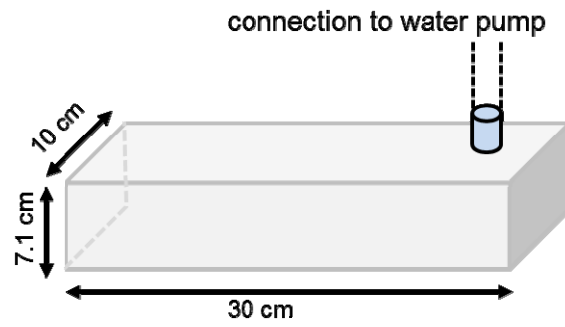
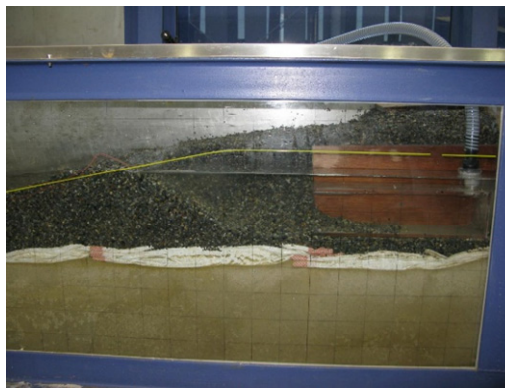


Figure 12. Shape of floodway mouth and connection with pump.

(a) Side view



(b) Overview



Figure 13. Side view and overview of wave flume.

Table 2. Cases of experiment.		
Case	Discharge	
	Experiment Q_m (ml/s)	Prototype Q_p (m^3/s)
1	0	0
2	17	0.3
3	34	0.6
4	68	1.2
5	102	1.8
6	136	2.4
7	170	3.0

RESULTS OF EXPERIMENT

Given a constant discharge from the floodway, waves were incident to the model beach of uniform slope. With the increase in water level in front of the mouth, filtration flow under the gravel beach occurred because of the difference between the inner water level and the mean sea level. Because the width of the floodway is one-fourth of the channel width, the effect of the filtration flow on the beach changes concentrated along the side wall, where the mouth was set, and its effect decreases with increasing distance from the side wall, suggesting the formation of a concave topography. In the experiment, therefore, the longitudinal profile along the side wall where the most dominant effect could be observed was measured.

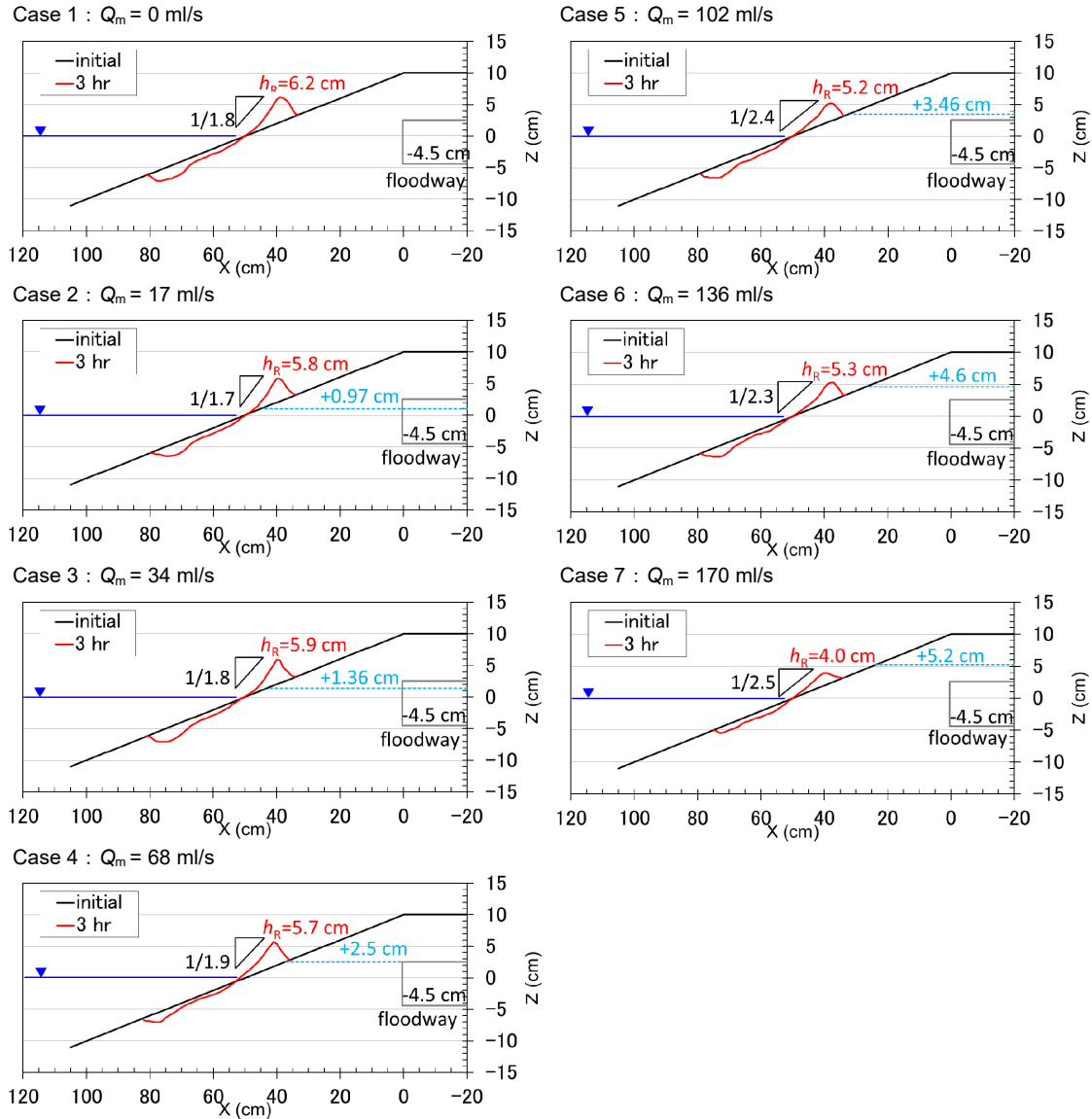


Figure 14. Longitudinal profiles in Cases 1-7 after 3-hour wave action.

Figure 14 shows the results of the experiment on berm formation with the existence of filtration flow and the change in longitudinal profile after a three-hour wave action in Cases 1–7, as well as the inner water level in front of the floodway. In Case 1 with no discharge, shoreward sand transport took place under the waves, and a berm of 6.2 cm height along with a foreshore slope of 1/1.8 was formed. This result gives a reference to other cases. In Case 2 with the discharge of $Q_m = 17$ ml/s, the berm height was 5.8 cm with a foreshore slope of 1/1.7. The berm height in Case 2 was reduced by 0.4 cm, but the change in foreshore slope was minimal. In Case 3 with the discharge of $Q_m = 34$ ml/s, the berm

height was 5.9 cm and the foreshore slope was 1/1.8; the berm height was reduced by 0.3 cm relative to that in Case 1, but there was no change in the foreshore slope. In Case 4, in which the discharge was further increased up to $Q_m = 68$ ml/s, the berm height was 5.7 cm, which decreased by 0.5 cm compared with that in Case 1, along with the decrease in the foreshore slope up to 1/1.9. In Case 5 with the discharge of $Q_m = 102$ ml/s, the berm height was 5.2 cm, which decreased by 1.0 cm. In addition, the foreshore slope became as gentle as 1/2.4. In Case 6 with $Q_m = 136$ ml/s, the berm height was 5.0 cm lower than that in Case 1 by 1.2 cm, and the foreshore slope was reduced to 1/2.3. Finally, in Case 7 with $Q_m = 170$ ml/s, the berm height was 4.0 cm lower than that in Case 1 by 2.2 cm and the gentle foreshore slope of 1/2.5 was formed. As mentioned above, it was found experimentally that the berm height and foreshore slope decreased with the increase in discharge. Table 3 shows all the measured results.

Case	Discharge Q_m (ml/s)	$\cot\beta$	berm height h_R (cm)	h_R/h_{R1}	Inner water level W_L (cm)
1	0	1.8	6.2	1	-
2	17	1.7	5.8	0.93	0.97
3	34	1.8	5.9	0.95	1.36
4	68	1.9	5.7	0.92	2.50
5	102	2.4	5.2	0.84	3.46
6	136	2.3	5.3	0.86	4.60
7	170	2.5	4.0	0.64	5.20

Figure 15 shows the relationship between the discharge Q_m (ml/s) and the inner water level W_L (cm) on the basis of the experimental results, as shown in Table 3. A relation was obtained.

$$W_L = 0.033 Q_m \tag{2}$$

W_L increased with the discharge, and the increase in the inner water level in turn intensified the filtration flow on the gravel layer. Figure 16 shows the relationship between the discharge Q_m and the ratio of the berm height h_R relative to that in Case 1 (h_R/h_{R1}). Between the two variables, a relation was obtained:

$$h_R/h_{R1} = 1.0 - 0.0016 Q_m \tag{3}$$

The berm height gradually decreased with the increase in the amount of discharge. Furthermore, the relationship between the reciprocal of the foreshore slope and the discharge Q_m is shown in Fig. 17 with the linear relation

$$\cot\beta = 1.79 + 0.004 Q_m \tag{4}$$

The foreshore slope and the berm height decrease with increasing Q_m , and these results are in good agreement with the observation results around the Shin-nakagawa floodway.

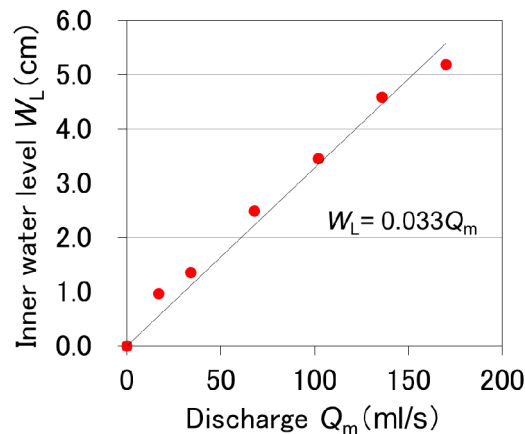


Figure 15. Relationship between Q_m and inner water level W_L .

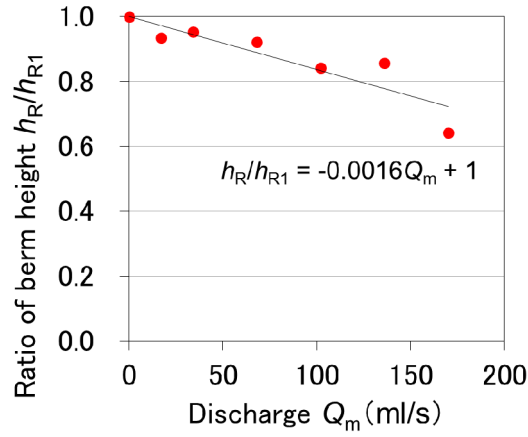


Figure 16. Relationship between Q_m and ratio of berm height relative to that in Case 1 (h_R/h_{R1}).

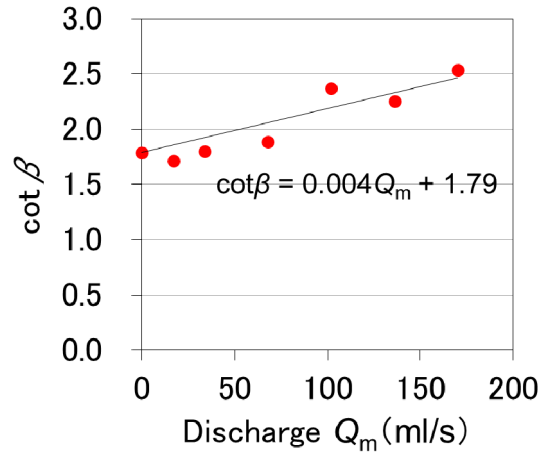


Figure 17. Relationship between Q_m and reciprocal of foreshore slope, $\cot\beta$.

NUMERICAL MODEL

The cross-shore sand transport under the condition that waves and seaward flow, such as filtration flow, coexist was derived. The cross-shore sand transport q_z is assumed to be given as a linear sum of the component due to waves, q_{zW} , and that due to seaward flow, q_{zR} , as Eq. (5).

$$q_z = q_{zW} + q_{zR} \quad (5)$$

Here, shoreward sand transport was assumed to be positive, and for the cross-shore sand transport q_z , the basic equation in the contour-line-change model proposed by Serizawa et al. (2003) was employed, as shown in Eq. (6).

$$q_{zW} = A_w \cdot \left(\frac{\cot \beta}{\cot \beta_c} - 1 \right) \quad (-h_c \leq z \leq h_R) \quad (6)$$

$$A_w = \varepsilon_z(z) \cdot K_z \cdot (EC_g)_b \cdot \sin \beta_c \quad (7)$$

Here, β is the angle of the seabed slope, β_c is the angle of the equilibrium slope, z is the water depth, h_c is the depth of closure, and h_R is the berm height. Beach changes can occur in the depth zone between h_c and h_R . The coefficient A_w given by Eq. (7) shows the intensity of sand transport due to waves and is proportional to the wave intensity. $\varepsilon_z(z)$ is the depth distribution function of the intensity of cross-shore sand transport, and in this study, we employed the depth distribution proposed by Uda and Kawano

(1996). K_z is the coefficient of cross-shore sand transport, and $(EC_g)_b$ is the energy flux of waves at the breaking point. By referring to the expression of the sand transport component due to waves as Eq. (2) and designating the sand transport component due to the seaward currents q_{zR} as $-A_R$, we obtain

$$q_{zR} = -A_R \quad (A_R > 0) \quad (8)$$

Here, Eq. (5) can be transformed to Eq. (9) using Eqs. (6) and (8).

$$q_z = A' \cdot \left(\frac{\cot \beta}{\cot \beta'_c} - 1 \right) \quad (9)$$

$$A' = \lambda A_w \quad (10)$$

$$\cot \beta'_c = \lambda \cot \beta_c \quad (11)$$

$$\lambda = 1 + A_R/A_w \quad (12)$$

Although Eq. (9) is similar to Eq. (6), the intensity of the sand transport and the equilibrium slope change as Eqs. (10) and (11) in response to the factor λ as Eq. (12). Without seaward currents ($A_R = 0$), λ is unity, and Eq. (9) agrees with Eq. (6). On the other hand, when the action due to the currents is intensified compared with that due to waves (larger A_R/A_w), λ takes a greater value than unity, and the equilibrium slope $\tan \beta'_c$ ($= 1/\cot \beta'_c$) decreases with a larger coefficient of intensity of sand transport (A'). The effect of the seaward currents on the cross-shore sand transport can be incorporated in this way as the change in equilibrium slope. In the calculation, we assumed that $\lambda = 1$ in a wave-dominated field, and the condition of $\lambda > 1$ was set when seaward currents are dominant, using the numerical model of the contour-line-change model as proposed by Serizawa et al. (2003). In this method, $\cot \beta_c$ and the intensity of sand transport A_w are increased by λ using Eqs. (11) and (10) where seaward currents dominate, and the numerical simulation considering the effect of seaward currents could be possible. λ is an additional correction factor. The calculation domain was discretized using the staggered meshes, and the sand transport rate was calculated using the cross-shore sand transport as Eq. (9) and the longshore sand transport equation. The beach changes were calculated explicitly by solving the continuity equation on the x - y plane by the explicit finite-difference method.

Because the width of the mouth is one-fourth of the channel width, three-dimensional (3-D) beach changes will occur, so 3-D numerical simulation was carried out. Assuming the initial berm height of 6 cm and the beach slope of 1/5, the calculation domain was discretized by $\Delta x = \Delta y = 2$ cm, and Δt was set as 1 s. The depth distribution of sand transport was assumed to be given by a uniform distribution throughout the depth, and the equilibrium slope was calculated from Eqs. (11) and (12). Table 4 shows the calculation conditions. The calculation was carried out by the 100-fold scale, and then the results were reduced by the factor of 1/100.

Numerical model	Contour-line change model (Serizawa et al. 2003)
Initial bathymetry	Straight, parallel contours with a slope of 1/5
Equilibrium slope	1/1.8 ($Z = 10$ -0 cm), 1/3.6 ($Z = 0$ -15 cm)
Wave conditions	Breaker height $H_b = 3.0$ cm
Depth of closure and berm height	Depth of closure $h_c = 6$ cm, Berm height $h_R = 6.2$ cm $h_c = 5$ cm, and $h_R = 4.0$ cm ($X = 0$ -10 cm) in Case 7
Coefficients of sand transport	Coefficient of longshore sand transport $K_y = 0.2$, Coefficient of cross-shore sand transport $K_z = 0.1K_y$
Depth distribution of sand transport	Cubic equation given by Uda and Kawano (1996)
Critical slope of falling sand	1/2 on land and seabed
Calculation range in depth	$z = 10.5$ - -15.5 cm
Calculation mesh	$\Delta X = 5$ cm, $\Delta Z = 1$ cm
Time intervals	$\Delta t = 0.0001$ h
Boundary conditions	$q_x = 0$ at landward and seaward boundaries and $q_y = 0$ at both ends
Remarks	Additional correction factor in Case 7: $\lambda = 1 + A_R/A_w = 1.4$ ($X = 0$ -10 cm, $Z = +4$ - -5 cm)

Figures 18 and 19 show the initial bathymetry and calculated bathymetry after a 3-hour wave action for Case 1 without $Q_m = 0$ and Case 7 with $Q_m = 170$ ml/s, respectively. In Case 1, shoreward sand transport occurred and sand was deposited near the shoreline with contours densely distributed between -6 cm and 6 cm heights. In Case 7 with $Q_m = 170$ ml/s, the concave contours on land and the convex contours on the seabed were formed in front of the area with seaward currents.

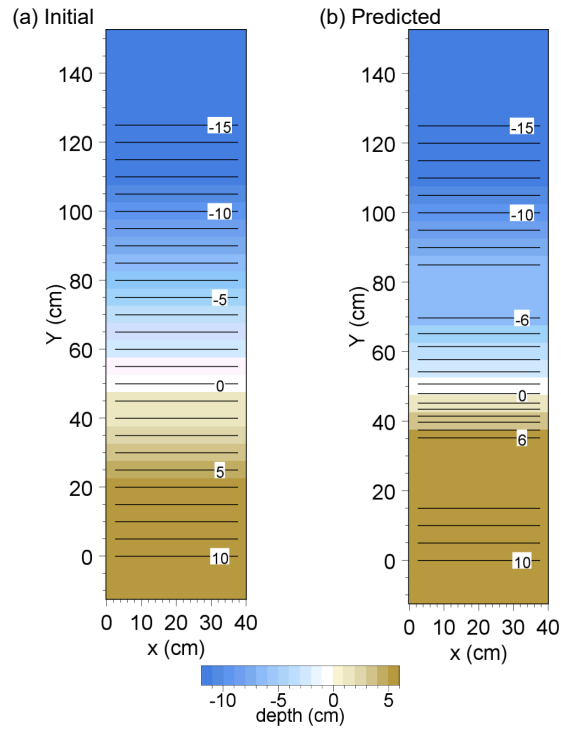


Figure 18. Bathymetric changes in Case 1.

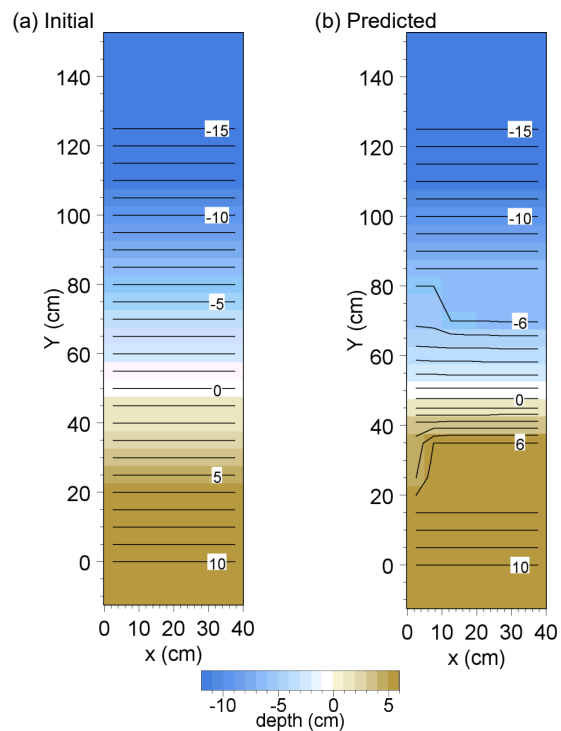


Figure 19. Bathymetric changes in Case 7.

Figure 20 shows the sand transport flux in Case 7. A circulation of sand transport from outside to the area with seaward currents along the shoreline and the return currents in the offshore zone was predicted. Thus, the concave bathymetry in front of the mouth of the floodway could be dynamically maintained, and these results explain the measured topography, as shown in Fig. 4 in front of the Shin-nakagawa floodway. Figure 21 shows the changes in longitudinal profiles in Cases 1 and 7. Although a berm was formed due to the shoreward sand transport in both cases, the berm height in Case 7 was reduced by 2.2 cm compared with that in Case 1, similarly to the experiment.

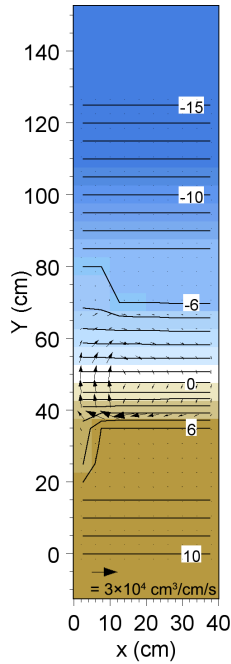


Figure 20. Sand transport flux in Case 7.

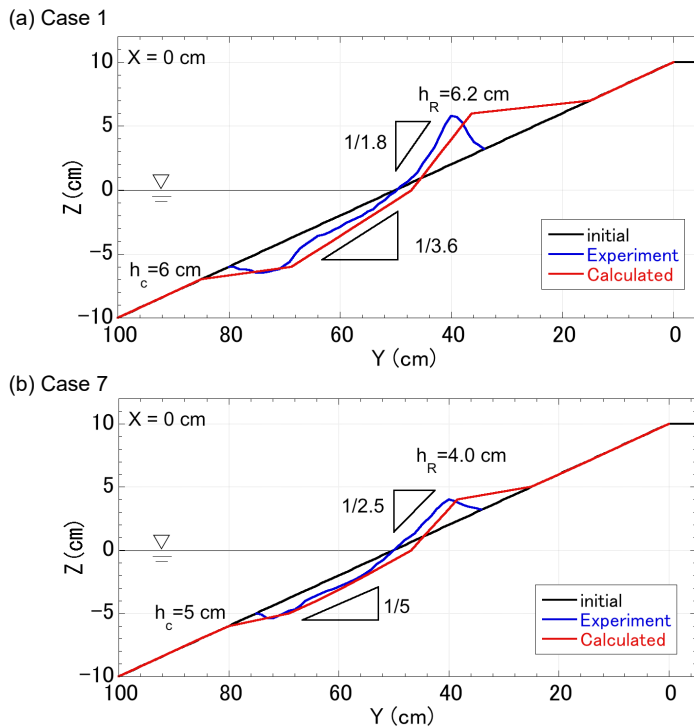


Figure 21. Longitudinal profiles (experiment vs. simulation).

CONCLUSIONS

In the experiment, gravel with a grain size of 3.3 mm was employed as the material. This grain size can be transformed as 16.5 mm in the prototype. The grain size of the bed material near the Shin-nakagawa floodway ranges from 5 to 10 cm, as shown in Fig. 5, and the grain sizes in the experiment and in the prototype drop in the same order of magnitude, and thus the phenomena observed at the Shin-nakagawa floodway can be explained by the results of the experiment. In the prototype and experiment, the grain size of the bed material is significantly large with a large velocity of the filtration flow. This weakened the wave action during incoming waves, resulting in reductions in the foreshore slope (equilibrium slope) and berm height. Finally, the effect of the filtration flow on the cross-shore sand transport was incorporated in the contour-line-change model, and calculation results were in good agreement with the experimental results.

REFERENCES

- Horikawa, K. ed. 1988. *Nearshore Dynamics and Coastal Processes*, University of Tokyo Press, Tokyo, 522p.
- Serizawa, M., T. Uda, T. San-nami, F. Furuike, and K. Kumada. 2003. Improvement of contour line change model in terms of stabilization mechanism of longitudinal profile, *Coastal Sediments '03*, 1–15.
- Shibasaki, M., T. Uda, M. Serizawa, T. Kumada, and A. Kobayashi. 2004. On the configuration of rip channel accelerating development of rip current, *Proceedings of 29th International Conference on Coastal Engineering*, ASCE, 1506–1518.
- Uda, T. and S. Kawano. 1996. Development of contour-line change model for predicting beach changes, *Proceedings of JSCE*, No. 539/II-35, 121–139. (in Japanese)